Kazan Federal University
Zavoisky Physical-Technical Institute

ACTUAL PROBLEMS OF MAGNETIC RESONANCE AND ITS APPLICATION

XXIV International Youth Scientific School

Program and Proceedings

Kazan
September 23-29, 2024

KAZAN FEDERAL UNIVERSITY
ZAVOISKY PHYSICAL-TECHNICAL INSTITUTE

ACTUAL PROBLEMS OF MAGNETIC RESONANCE AND ITS APPLICATION

XXIV International Youth Scientific School

Program and Proceedings

Kazan
September 23–29, 2023

KAZAN
2024

UDC 537
LBC 22.334
A19

Administration of the School:

E.M. Alakshin (KFU, Kazan) — rector;
M.S. Tagirov (KFU, Kazan) — scientific adviser;
Y.I. Talanov (KFTI RAS, Kazan) — vice-rector;
V.K. Voronkova (KFTI RAS, Kazan) — vice-rector;
A.S. Makarchenko (KFU, Kazan) — vice-rector

Program committee:

Professor M.R. Gafurov (KFU, Kazan);
Professor L.R. Tagirov (KFU, Kazan);
Professor M.S. Tagirov (KFU, Kazan);
Associate professor Alakshin E.M. (KFU, Kazan)

Organizing committee:

E.M. Alakshin, A.S. Makarchenko,
E.I. Boltenkova, I.V. Romanova

A19 **Actual problems of magnetic resonance and its application [Electronic resource]:** program and proceedings of the XXIV International Youth Scientific School (Kazan, September 23–29, 2024) / edited by E.I. Boltenkova, E.M. Alakshin. – Electronic text data (1 file: 33 Mb). – Kazan: Kazan University Press, 2024. – 30 p. – System requirements: Acrobat Reader. – Access mode: http://apmra-kzn.com/proceedings/mrschool2024.pdf. – Heading from title screen.

ISBN

This collection contains the reports of young scientists submitted to the XXIIII International Youth Scientific School “Actual problems of magnetic resonance and its application”, organized by the Kazan Federal University and the Zavoisky Physical-Technical Institute.

The cover design was developed by D.A. Tayurskii.

UDC 537
LBC 22.334

ISBN

Monday, September 23

08:30 – 10:00 Registration

Thursday, September 26

09:00 – 10:30 Plenary lectures (EPR-80)

10:30 – 11:00 **Coffee break**

11:00 – 11:15 Opening Ceremony

11:15 – 11:30 A**.M. Garaeva**, "Study of magnetic properties for DyF_3 particles"

11:30 – 11:45 **A.P. Yi**, "NMR signal amplification by reversible exchange (SABRE) of nitroimidazole antibiotics at microtesla magnetic fields"

11:45 – 12:00 **Yu.V. Slesareva**, "Molecular Dynamics of Acetonitrile Intercalated into Graphite Oxide Studied via ^1H NMR"

12:00 – 12:15 **U.V. Bulgakova**, "NMR metabolomics study of "Normoflorin" treatment effects on patients with chronic kidney disease"

12:15 – 12:30 **B.M. Mukhamadullin**, "Study of paramagnetic centers in lanthanum trifluoride nanoparticles by EPR"

12:30 – 13:30 **Lunch**

13:30 – 13:45 **A. R. Sadykov**, "Implementation of Hadamard operator by non-resonant RF pulse and one spin qubit"

13:45 – 14:00 **D.A. Makarov**, "Spin Hall effects in thin film Py/Pt heterostructure"

14:00 – 14:15 **A.V. Shestakov,** "Magnetic properties of $La_{1-y}Sr_yMn_{0.9}Fe_{0.05}Zn_{0.05}O_3$ (y = 0.17, 0.19, 0.3)"

14:15 – 14:30 **A.V. Shestakov**, "Study of the magnetic properties of PbTe (Mn,Cu) by ESR method in X, Q, V-bands"

14:30 – 14:45 **A.I. Shamsieva**, "Computer design of 2D organic materials for lithium-ion batteries"

14:45 – 15:00 **A.A. Evseev**, "*Ab initio* study of heterostructures based on ferroelectric and metal for spintron applications"

15:00 – 15:30 **Coffee break**

15:30 – 15:45 **Z.K. Pulotov**, "Spin-Hall effects in heteroepitaxial structure $Pd_{0.88}Fe_{0.12}$/Pt"

15:45 – 16:00 **A.Kh. Kadikova**, "Magnetic inhomogeneities in Fe_3Al epitaxial thin films probed by FMR and time-resolved magnetooptics"

16:00 – 16:15 **A.V. Popov**, "Combined equation of semiclassical spin dynamics and electron paramagnetic resonance"

16:15 – 16:30 **F.M. Siraev**, "Description of unconventional superconductivity in the regime of strong fluctuations"

16:30 – 16:45 **R.A. Podarov**, "Dipolar EPR Spectroscopy of Fullerene and Porphyrin Symmetric Pairs"

16:45– 17:00 **A.A. Petrova**, "EPR investigations of composite materials based on biocompatible polymers with calcium phosphates"

17:00 – 17:15 **T.N. Enderova**, "Non-resonant microwave absorption in topological insulator $Bi_{1.1-x}Sn_xSb_{0.9}Te_2S$"

Friday, September 27

12:30 – 13:30 Closing Ceremony

Study of magnetic properties for DyF_3 particles

A.M. Garaeva, I.V. Romanova, G.Yu. Andreev, E.I. Boltenkova, E.M. Alakshin

Institute of Physics, Kazan Federal University, Kazan, Russian Federation

e-mail: adeliagaraeva84@gmail.com

The DyF_3 compound has unique properties, which makes it possible to use it as a high-field contrast agent for MRI [1] and additives to Nd-Fe-B magnets to increase the coercive force [2]. Dysprosium fluoride is a ferromagnet with an easy magnetization axis along the [010] axis of the crystal lattice; the space symmetry group is Pnma (orthorhombic); the Curie temperature is 2.55 K along the [010] axis for a single crystal [3].

DyF_3 powders with characteristic sizes of 30 nm x 16 nm, 50 nm x 30 nm, 70 nm x 40 nm, 220 nm x 150 nm were obtained by hydrothermal synthesis via chloride reaction [4], powder size of 7 μm x 5 μm – by crushing a single crystal. Chemical composition control and crystallinity confirmation were carried out using X-ray diffraction analysis on Bruker D8 Advance Cu Ka, λ=1.5418 Å. The shape and characteristic size of the particles in the powders were determined from photographs obtained using transmission electron microscopy on a HitachiHT Exalens microscope.

In this work, magnetic field (0 – 7 T) dependences of magnetization of samples were measured using the magnetic properties measurement system (Quantum Design), St. Petersburg State University, as well as temperature dependences of heat capacity in fields up to 9 T on a multifunctional system for measuring physical properties with a superconducting magnet PPMS-9, Kazan Federal University. The modeling of the energy spectrum and magnetization was carried out in the charge exchange model in the full basis of the electron configuration of Dy^{3+} $4f^9$ in DyF_3. It was obtained that the powder is magnetically ordered. The particles are clustered so that the easy magnetization axis is directed mainly along the external magnetic field. The saturation value of the magnetic moment in strong magnetic fields changes with decreasing particle size. It is shown that the change in magnetization is due to surface effects and clustering.

The work was carried out by the Russian Science Foundation (Project No. 23-72-10039).

[1] D. González-Mancebo et al., Particle & Particle Systems Characterization **34**, 1700116 (2017).
[2] F. Xu et al., Scripta Materialia **64**, 1137 (2011).
[3] A.V. Savinkov et al., Journal of Physics: Condensed Matter **20**, 485220 (2008)
[4] Yi G. S., Chow G. M. Journal of Materials Chemistry **15**, 4460-4464 (2005)

NMR signal amplification by reversible exchange (SABRE) of nitroimidazole antibiotics at microtesla magnetic fields

A.P. Yi[1,2], O.G. Salnikov[1], D.B. Burueva[1], N.V. Chukanov[1], I.V. Koptyug[1]

[1]International Tomography Center SB RAS, Novosibirsk, Russia
[2]Novosibirsk State University, Novosibirsk, Russia

e-mail: anna.i@tomo.nsc.ru

SABRE-SHEATH approach provides a significant increase of heteronuclear NMR signal by reversible binding of both parahydrogen and substrate molecules to an Ir complex in ultralow magnetic field. Ones of the most promising substrates for SABRE-SHEATH hyperpolarization are metronidazole and nimorazole antibiotics. They serve as hypoxia radiosensitizers and have prospects for application as MRI contrast agents for cancerous tumor visualization. In the previous SABRE-SHEATH studies of isotopically enriched [$^{15}N_3$]metronidazole and [$^{15}N_3$]nimorazole, methanol-d_4 was used as a solvent [1, 2]. Nevertheless, more available nondeuterated solvents, such as methanol and ethanol (the latter one is more biocompatible than methanol-d_4), are more preferable choice for potential utilization of this method in medicine. Herein, we investigated the impact of solvent nature on SABRE-SHEATH performance and ^{15}N hyperpolarization lifetimes of [$^{15}N_3$]metronidazole and [$^{15}N_3$]nimorazole and also defined optimal conditions of polarization transfer.

The key parameters of SABRE-SHEATH experiments are the polarization transfer field and the temperature. We started with the measurements of magnetic field profiles at 4 different temperatures with a 10 °C increment. Further temperature sweeps were obtained at previously optimized magnetic field. As a result, for [$^{15}N_3$]metronidazole, the maximal ^{15}N polarization was observed at ~23 °C and 0.72 μT in methanol and at ~23 °C and 0.67 μT in ethanol. The optimal parameters for [$^{15}N_3$]nimorazole were 43 °C and 0.55 μT in methanol and 33 °C and 0.62 μT in ethanol. The obtained data are in a good agreement with the previous results [1, 2]. Pressure, flow rate sweeps, polarization buildup and decay profiles were measured at the identified optimal conditions. Also relaxation times at clinically relevant 1.4 T magnetic field were obtained. The longest polarization decay times were observed for the nitro group of [$^{15}N_3$]metronidazole and [$^{15}N_3$]nimorazole in methanol and ethanol, respectively, and made up about several minutes. The maximum attainable averaged polarization for metronidazole decreased from CD_3OD ($P_{15N,max}$ = 7.6%) to CH_3OH ($P_{15N,max}$ = 6.1%) and to C_2H_5OH ($P_{15N,max}$ = 4.7%). For [$^{15}N_3$]nimorazole, the highest polarizations were observed in C_2H_5OH ($P_{15N,max}$ = 7.65%), while CH_3OH and CD_3OD provided similar polarization levels ($P_{15N,max}$ of 6.1% and 5.8%, respectively).

One more member of the group of nitroimidazole antibiotics, which was not studied earlier, is ^{15}N-enriched ornidazole. Herein, we found that optimal conditions for SABRE-SHEATH hyperpolarization of [$^{15}N_3$]ornidazole are close to those of [$^{15}N_3$]metronidazole (0.62 μT field and 23 °C temperature). Polarization lifetimes for [$^{15}N_3$]ornidazole at 1.4 T (~450 s) compared favorably with those of [$^{15}N_3$]metronidazole (~230 s). Nevertheless, the maximum attainable ^{15}N polarizations for [$^{15}N_3$]ornidazole were somewhat lower (5.40%).

This work was supported by the Russian Science Foundation (grant 24-73-10093).

[1] O.G. Salnikov et al., Angew. Chem., Int. *Ed.* **60**, 2406 (2021).
[2] J.R. Birchall et al., Chem. Commun. **56**, 9098 (2020).

Molecular Dynamics of Acetonitrile Intercalated into Graphite Oxide Studied via ^{1}H NMR

Yu. Slesareva[1], M. Volkov[1], E. Vavilova[1], D.A. Astvatsaturov[2,3], N. Chumakova[2,3]

[1] Zavoisky Physical-Technical Institute, FRC Kazan Scientific Center of RAS, Kazan, Russia
[2] N. N. Semenov Federal Research Center for Chemical Physics, Russian Academy of Science, Kosygin St. 4, Moscow, 119991, Russia
[3]M.V. Lomonosov Moscow State University, Chemistry Department, Leninskiye Gory, 1/3, Moscow 119991, Russia

e-mail: yulia.slesarev@gmail.com

Graphite oxide (GO) consists of layered graphene planes with attached oxygen-containing groups. GO and its derivatives are promising as materials for membranes for liquid and gas purification and separation due to their layered structure and functional properties. However, the molecular mobility of substances within the oxidized graphene layers, which is crucial for understanding the permeability mechanism of these membranes, is still not well understood.

This study focuses on investigating the molecular mobility of graphite oxide samples containing various amounts of intercalated acetonitrile using ^{1}H nuclear magnetic resonance (NMR) spectroscopy. By analyzing the temperature-dependent ^{1}H NMR spectra of the samples, we have estimated the activation energy of the acetonitrile molecules. The spectra show that as the temperature increase, the spectral lines narrow and distinct side signals become more pronounced. Experiments conducted using magnetic fields of varying strengths indicated no alteration in the splitting value, implying that the side signals likely originate from dipole-dipole interactions rather than the presence of distinct signals. Through computational modeling of the spectra, we have gained a deeper insight into the molecular dynamics of the acetonitrile intercalated in GO.

The nuclear magnetic resonance measurements were performed with the financial support from the government assignment for FRC Kazan Scientific Center of RAS.

NMR metabolomics study of “Normoflorin” treatment effects on patients with chronic kidney disease

U.V. Bulgakova[1], S.S. Mariasina[1], O. Gavrilova[1], A.G. Kuzmina[1], S.A. Bolshakov[1], V.A. Ivlev[3], E.V. Shutov[3], V. Polshakov[1]

[1] Lomonosov Moscow State University, Moscow, Russia
[2] Botkin Hospital, Moscow, Russia
[3] RUDN University, Moscow, Russia
email: uliana-bulgakova@mail.ru

Chronic kidney disease (CKD) is a progressive condition characterized by the gradual loss of kidney function, leading to the accumulation of waste products and alterations in metabolic processes. The gut microbiome has been implicated in the pathophysiology of CKD, with dysbiosis contributing to the accumulation of uremic toxins and exacerbating the disease. In recent years, probiotic supplementation has been used as an adjuvant therapy in CKD, and several studies have shown that probiotics influence the progression of CKD by altering the gut flora and reducing uremic toxins [1]. The aim of this study was to investigate the effect of treatment with “Normoflorin”, a prevalent probiotic drug, on the blood metabolic profile of patients with CKD using nuclear magnetic resonance (NMR) approach.

The study included 60 patients diagnosed with CKD who were undergoing peritoneal dialysis. Participants were divided into two groups: one group received “Normoflorin” for 1 month (N=38) and the other group did not (N = 22). Blood serum samples were collected from each participant at baseline and after the treatment period. ^{1}H NMR spectroscopy was utilized to analyze the serum samples, focusing on low-molecular-weight metabolites.

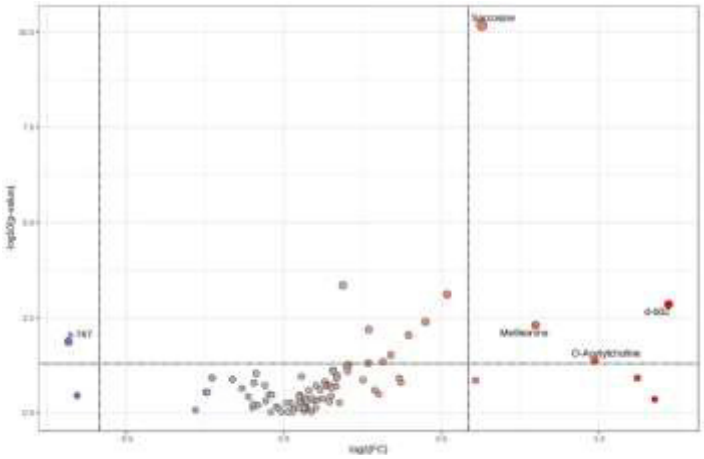

Fig1. Volcano plot of paired comparison metabolites before and after Normoflorine treatment

A total of 55 metabolites were identified in serum samples from patients with CKD. The t-test demonstrated statistically significant changes in several metabolites following “Normoflorin” treatment, including sarcosine, fumarate, hypoxanthine, methionine, isobutyrate, ornithine, acetylcholine and pyruvate (Fig. 1). The PLS-DA analysis revealed differences in hippurate and creatinine concentration. Furthermore, there was a notable tendency towards elevated levels of sarcosine, methionine, pyruvate, isobutyrate and acetylcholine. These findings indicate that “Normoflorin” therapy induces specific metabolic alterations in patients with CKD, predominantly impacting amino acid metabolism and, to a lesser extent, glycerophospholipid metabolism and the TCA cycle. Although no significant changes in investigated uremic toxins (Indoxyl Sulfate, TMAO, hippurate) were detected, the observed metabolic changes offer insights into the potential therapeutic mechanisms of “Normoflorin” in the management of CKD.

This research was funded by grant from the Moscow government (research project No. 1803-7/23)

Study of paramagnetic centers in lanthanum trifluoride nanoparticles by EPR

B.M. Mukhamadullin, E.M. Alakshin, A.M. Garaeva, E.I. Boltenkova, F.F. Murzakhanov, G.V. Mamin

Institute of Physics, Kazan Federal University, Kazan, Russian Federation

e-mail: bulatm4635@gmail.com

Lanthanum trifluoride LaF_3 nanoparticles are interesting to study due to the magnetic properties that is not characteristic of bulk crystal. LaF_3 has a hexagonal crystal lattice with space group P3c1 [1]. The electrons of the outer shell of lanthanum ions interact with electrons of fluorine ions, which leads to the splitting of energy levels corresponding to different orbital states. As a result of this interaction, all electrons in the outer shell of lanthanum ions are paired. A LaF_3 monocrystal is diamagnetic and does not have unpaired electrons [2]. However, recent studies [3] observed an electron paramagnetic resonance (EPR) signal in LaF_3 nanoparticles doped with Pr^{3+} ions, and the position of the line did not correspond to the g-factor of the impurities.

In this work, LaF_3 nanocrystals were synthesized using coprecipitation methods with hydrothermal treatment in an autoclave for 24 hours at temperatures of 120°C, 160°C and 230°C. Crystallinity and the chemical composition were estimated using X-ray diffraction analysis on a Bruker D8 Advance Cu Kα (λ = 1.5418 Å) and mass spectrometry with inductively coupled plasma on an iCAP Qc (ThermoFisher Scientific, Germany). Transmission electron microscopy (Hitachi HT7700 Exalens, accelerating voltage of 100 keV) images were recorded to determine the shape and the particles size.

ESR spectra of series LaF_3 nanoparticles without doping impurities were measured using Bruker Elexsys E580 in X band (9.6 GHz) at room temperature. A complex-shaped electron paramagnetic resonance line for all nanoparticle samples was observed. The number of paramagnetic centers (PCs) was estimated; $Cu^{2+}(DETC)_2$ dissolved in toluene with a spin concentration of 2.44 mol/L was used as a marker. An increase of paramagnet center concentration was found with increasing temperature of hydrothermal treatment. A model with paramagnetic centers in core and shell of nanoparticles is proposed and is in good agreement with the experimental results. Further study of this effect is required to identify the nature of PCs and the conditions for their occurrence.

This work was supported by the Russian Science Foundation (Project No. 23-72-10039).

[1] M. Mansmann, Zeitschrift für anorganische und allgemeine Chemie **331**, 98 (1964).
[2] E. Talik et al., Journal of alloys and compounds **616**, 556 (2014).
[3] M.S. Pudovkin et al., Materials Chemistry and Physics **294**, 127037 (2023).

Implementation of Hadamard operator by non-resonant RF pulse and one spin qubit

A. R. Sadykov, M. R. Arifullin

Faculty of Physics, Orenburg State University, Orenburg, Russian Federation

e-mail: aleksandr.sadykov.2012@mail.ru

The Hadamard transform is one of the most important operations in quantum computing [1]. The Hadamard operator is usually represented by a 2×2 matrix, which in the representation of spin operators has the form

$$H_{\mathrm{A}} = 2^{-1/2}\left(\sigma_x + \sigma_z\right) \tag{1}$$

The physical implementation of this operation using the spin states of electrons or nuclei in a magnetic field involves the use of two or more radio frequency pulses [2], the frequency of which ω is equal to the precession frequency ω_0. The effects of resonant pulses on spin systems are described in detail in [3,4].

The use of non-resonant pulses was shown to allow performing the Hadamard operation using only one pulse. In a non-resonant pulsed RF field with a frequency of ω_Γ and in a rotating coordinate system, the spin evolution is described by the operator

$$H = \left\{\left(\omega_0 - \omega_\Gamma\right)\sigma_z + \omega_1\sigma_x\right\}, \tag{2}$$

which for $\omega_0 - \omega_\Gamma = \omega_1$, takes the form of the Hadamard operator. The physical consequences of the action of such single non-resonant RF pulses are discussed.

[1] M.A. Nielsen, I.L. Chuang, Quantum computation and quantum information. Cambridge university press, 676 (2010).
[2] L.M. Vandersypen, I.L. Chuang, Reviews of modern physics **76**, 1037 (2004).
[3] T.C. Farrar, E. D. Becker, Pulse and Fourier transform NMR: introduction to theory and methods. Elsevier, 118 (2012).
[4] R.R. Ernst, G. Bodenhausen, A. Wokaun, Principles of nuclear magnetic resonance in one and two dimensions. Oxford university press (1990).

Spin Hall effects in thin film Py/Pt heterostructure

D.A. Makarov[1], A.Kh. Kadikova[1], A.I. Gumarov[1], I.V. Yanilkin[1], B.F. Gabbasov[1], A.V. Petrov[1], L.R. Tagirov[1,2], R.V. Yusupov[1]

[1]Institute of Physics, Kazan Federal University, Kazan, Russian Federation
[2]Zavoisky Physical-Technical Institute, Kazan, Russian Federation

e-mail: dmamakarov@stud.kpfu.ru

Spintronics, being a field of electronics that utilize a spin angular momentum of electron additionally to its electric charge, is interested in spin current generation, detection and manipulation techniques. The spin Hall effect is of great interest as a method that allows one to generate and detect spin currents via electric ones. However, there is a large discrepancy in determination of spin-charge conversion efficiency — spin Hall angle — for the same materials even with similar experimental setups [1, 2].

In this work spin Hall effects driven by spin pumping in Py/Pt heterostructure have been studied to determine the spin Hall angle of platinum. Samples have been prepared using molecular-beam epitaxy and magnetron sputtering for platinum and permalloy layers, respectively. Magnetic properties of Py thin film and Py/Pt heterostructure have been studied using vibrating sample magnetometry, ferromagnetic resonance and time-resolved magnetooptic Kerr effect. Saturation and remanent magnetization, coercive field, gyromagnetic ratio and constant of magnetic anisotropy perpendicular to plane of Py films have been determined. Gilbert damping constant of our samples as well as spin pumping contribution have been measured by two independent techniques, namely time-resolved magnetooptic Kerr effect and ferromagnetic resonance, in order to prove the validity of conducted measurements. Spin transport in Py/Pt heterostructure has been studied in order to determine spin Hall angle by using an inverse spin Hall effect induced by the spin pumping. Spin Hall angle has been calculated using theoretical model developed in [3].

We obtain spin Hall angle falling within the previously reported span of values for platinum [1, 2], moreover it lies near to the upper boundary. Another important result has been obtained from the investigation of an influence of inhomogeneous photoexcitation at a probe area as an upper boundary of relation between pump and probe spot sizes that is necessary for obtaining correct estimate of Gilbert damping constant using the time-resolved magnetooptic Kerr effect.

[1] J. Sinova et al., Rev. Mod. Phys. **87**, 1213 (2015).
[2] M. Weiler et al., Solid State Physics: Advances in Research and Applications **64**, 123 (2013).
[3] K. Ando et al., J. Appl. Phys. **109**, 103913 (2011).

Magnetic properties of $La_{1-y}Sr_yMn_{0.9}Fe_{0.05}Zn_{0.05}O_3$ (y = 0.17, 0.19, 0.3)

A.V. Shestakov[1], Z.Y. Seidov[2], I.V. Yatsyk[3], A.S. Ovchinnikov[4], F.G. Vagizov[5], V.A. Shustov[3], A.G. Badelin[6], V.K. Karpasyuk[6], H.-A. Krug von Nidda[7], R.M. Eremina[3]

[1] Prokhorov General Physics Institute of the RAS, Moscow, Russia
[2] Institute of Physics, Ministry of Science and Education, Baku, Azerbaijan
[3] Zavoisky Physical-Technical Institute, FRC Kazan Scientific Center of RAS, Kazan, Russia
[4] Institute of Natural Sciences and Mathematics,Ural Federal University, Ekaterinburg, Russia
[5] Institute of Physics, Kazan Federal University, Kazan, Russia
[6] Astrakhan State University, Astrakhan, Russia
[7] Experimental Physics V, Center for Electronic Correlations and Magnetism, University of Augsburg, Augsburg, Germany

e-mail: AlekseiVShestakov@gmail.com

Magnetic properties of polycrystalline $La_{1-y}Sr_yMn_{0.9}Fe_{0.05}Zn_{0.05}O_3$ (y = 0.17, 0.19, 0.3) have been investigated by means of electron spin resonance, magnetic susceptibility, and Mössbauer measurements. All samples show a clear ferromagnetic transition. The Curie temperature T_C increases on increasing Sr-ions content (Table 1). For all three samples, an anomalous downturn of the inverse susceptibility significantly above T_C and the concomitant observation of ferromagnetic resonance signals coexisting with the paramagnetic resonance up to approximately room temperature, indicates a Griffiths-like behavior [1, 2] (Fig. 1).This regime is characterized by the coexistence of ferromagnetic entities within the globally paramagnetic phase. Mössbauer studies indicate that Fe in these compounds is in the trivalent high-spin state. The temperature evolution of the Mössbauer spectra at low temperatures ($T < T_C$) is typical for ferromagnetic clusters with a wide distribution in size and magnetic correlation length.

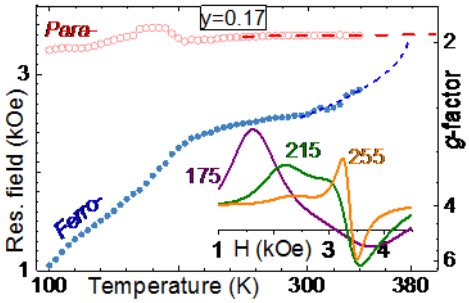

Tab. 1. Magnetic, magnetocaloric parameters.

y	T_C, K *Ref.*	T_C, K *c.i.*	$\|\Delta S_{max}\|$, J/(kg·K)	RCP, J/kg
0.3	278	277	**2.90**	**248**
0.19	222 [2]	216	**2.77**	**289**
0.17	208 [1]	204	**2.56**	**305**

We also observed a magnetocaloric effect with a maximum magnetic entropy change ($|\Delta S_{max}|$) values occurring close to the Curie temperature T_C and the relative cooling power (RCP) corresponding to values in Table 1 under magnetic field change (ΔH) of ~ 50 kOe. The critical properties of all samples were investigated by analysis of the magnetization measurements in the vicinity of their critical temperature. By means of Arrott plots, the nature of the magnetic transition is found to be of second order. The critical exponents β, γ and δ were evaluated using modified Arrott plots (MAP) [3] (Fig 2). The values of the critical exponents for the doped compounds are in fair agreement with the 3D-Heisenberg model.

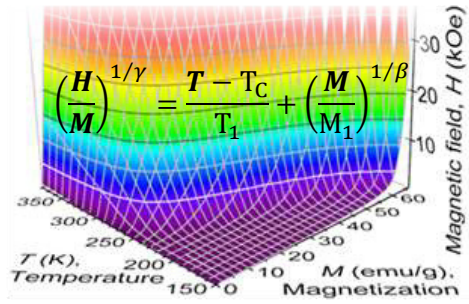

Fig. 2. *H-M-T*-plot (y = 0.19).

[1] Z.Y. Seidov, I.V. Yatsyk et.al, J. Magn. Magn. Mater. **552**, 169190 (2022).
[2] R.M. Eremina, I.V. Yatsyk et.al, Appl. Magn. Reson. **54**, 449-461 (2023).
[3] Arrott A. and Noakes J. E. Phys. Rev. Lett. **19**, 786 (1967).

Study of the magnetic properties of PbTe (Mn, Cu) by ESR method in X, Q, V-bands

A.V. Shestakov[1], I.V. Yatsyk[2], I.I. Fazlizhanov[2], A.V. Semeno[1], S.V. Demishev[3], V.A. Ulanov[2, 4]

[1] Prokhorov General Physics Institute of the Russian Academy of Sciences, Moscow, Russia
[2] Zavoisky Physical-Technical Institute, FRC Kazan Scientific Center of RAS, Kazan, Russia
[3] Institute for High Pressure Physics of the RAS, Troitsk, Moscow, Russia
[4] Kazan State Power Engineering University, Kazan, Russia
e-mail: AlekseiVShestakov@gmail.com

The PbTe direct narrow band semiconductor belongs to the group of lead chalcogenides with the cubic rock salt structure and strong ionic character. It has a positive temperature coefficient of the gap width, the high static dielectric constant, and the large carrier mobility. They make it unique among polar compounds and make it important applications in many fields, such as infrared detectors, light-emitting devices, infrared lasers, thermoelectric materials and solar energy panels. A small number of studies of quantum wires, dots, and wells in the PbTe semiconductor have been carried out using the ESR method. Because the most of the paramagnetic impurity centers form resonant levels in the conduction or valence band in the lead chalcogenides and all such centers are not observable by ESR method. It was found [1, 2] that the Mn^{2+} ions embedded in PbTe are well localized at the Pb sites and form local magnetic moments. Owing to the direct exchange interaction between the *d*-electrons and Bloch electrons of the valence and conducting bands, the latter are magnetically polarized. The manganese impurity centers can be used as paramagnetic probes to study some physical properties of PbTe semiconductors. We report here the X-band (~ 9.36 GHz) and Q-band (~ 34 GHz) and V-band (~ 60 GHz) ESR data (Fig. 1) on deep Mn^{2+} centers in PbTe (Mn, Cu) crystalline sample ($x_{Mn} \approx 0.0005 \div 0.001$) grown by vertical Bridgman method in quartz crucibles. This low concentration of Mn ions was chosen with the aim that the impurity ions work as a probe. Microwave absorption (in V-band) and its first derivative (in X and Q-band) were obtained at temperatures from 4.2 to 40 K and various angles. Sample was located vertically in the central part of the rectangular resonator (X-band) and cylindrical resonator (Q and V-band) at the antinode of the magnetic component. Six principal Mn^{2+} hyperfine lines (A=165÷202 MHz) were observed in the ESR spectra. The field intervals between the lines were found to be isotropic under rotation in the (100) plane within the experimental error of ~1 Oe. The EPR broad line with H_{res}~12.75 kOe was observed presumably from Cu ions. Quantum oscillations due to the de Haas-van Alphen effect were observed in all MW-bands. Similar to works [3, 4], it was established that the period of which increases with increasing magnetic field. The charge carrier concentration $81 \pm 14 \times 10^9$ cm^{-2} and effective mass $0.0042 m_e$ was estimated. All experimental facts observed in this study are discussed. The financial support was provided by the Prokhorov General Physics Institute of the RAS and FRC KazSC of RAS.

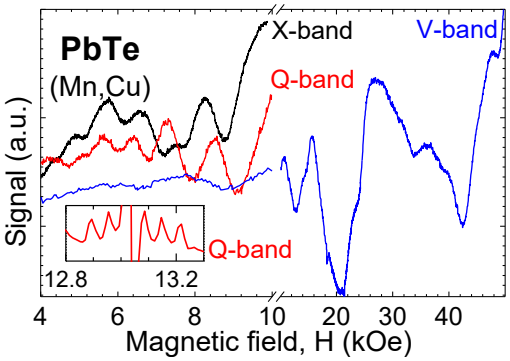

Fig. 1.: A series of ESR spectra of the sample in X, Q and V-band (T=4.2 K).

[1] V.-C. Lee, Phys. Rev. B **34**, 5430 (1986).
[2] J.H. Pifer, Phys. Rev. **157**, 272 (1967).
[3] A.V. Shestakov, I.I. Fazlizhanov et.al., IEEE Magnetics Letters **11**, 2503505 (2020).
[4] Y. Wang et.al., Scientific Reports **6**, 31554 (2016).

Computer design of 2D organic materials for lithium-ion batteries

A.I. Shamsieva, I.I. Gumarova, O.V. Nedopekin, D.A. Tayurskii

Institute of Physics, Kazan Federal University, Kazan, Russian Federation

e-mail: aigul-shamsieva@mail.ru

In today's world, high-performance batteries that can withstand high charges, have a long service life and remain stable are very important. One promising option is the use of porous organic polymers, which offer advantages such as light weight, flexibility, environmental friendliness, stability and ease of structure optimization. Covalent organic frameworks are environmentally friendly, have controlled theoretical capacitances and redox potentials, which makes them attractive as electrode materials. They can play an important role in electrode development due to their flexible structure, permeable framework, and diverse functional groups.

Li-ion batteries (LIBs) are considered extremely promising for electrical energy storage systems. However, there are certain challenges in choosing anode materials with higher conductivity and longer cycle life for practical applications. In this work, a novel two-dimensional (2D) porous monolayer, namely F,Si-co-doped covalent triazine framework (F,Si@CTF0), was designed using density functional theory (DFT) calculations. The results demonstrated that the co-doping of F and Si atoms on the CTF0 surface creates more accessible adsorption sites for Li-ion adsorption. The energy analysis confirmed the stability of the F,Si@CTF0 monolayer, which exhibits a notable adsorption energy (-3.53 eV) for Li-ion at site A (between Si and F atoms). The F,Si@CTF0 monolayer can potentially accommodate five Li-ions, providing a high theoretical specific capacity of 462 mAh g^{-1} (comparable to the graphite anode commonly employed in commercial LIBs) and a positive redox potential of 2.9 V. The adsorption of Li-ion transforms the F,Si@CTF0 monolayer from being semiconducting to metallic, reflecting high electronic conductivity. Moreover, the monolayer undergoes minor lattice variations (-1.3%) throughout the lithiation/delithiation process, demonstrating excellent cycling performance. Finally, Li-ion diffuses rapidly on the surface of the monolayer with a small diffusion energy barrier of 0.078 eV. These results highlight the potential use of the F,Si@CTF0 monolayer as a promising anode material for the next-generation LIBs.

[1] X. Lv, Phys. Chem. Chem. Phys. **22**, 8902 (2020).
[2] J. Xu, Science China Chemistry **64**, 1267 (2021)

Ab initio study of heterostructures based on ferroelectric and metal for spintron applications

A.A. Evseev, I.I. Gumarova, O.V. Nedopekin

Institute of Physics, Kazan Federal University, Kazan, Russian Federation

e-mail: alexander-alexandrovich-evseev@mail.ru

Materials utilized in spintronic devices and for detecting Majorana fermions in solids require significant and optimal Rashba-type spin-orbit splitting. Recently, a new approach has been proposed, combining ordered surface fusion with interface engineering—specifically, the growth of alloy monolayers on a polar insulating surface [1]. The Rashba effect refers to spin-orbit splitting at surfaces or interfaces resulting from the breaking of inversion symmetry [2].

In this study, we investigated film heterostructures with various component combinations that are anticipated to exhibit Rashba-type spin-orbit splitting [2, 3]. The presence of an electron density gradient at the interfaces leads to an eddy current linked to electron spins. We explored the structural and electronic properties of these systems, performing electronic calculations using DFT+U to account for spin-orbit interactions. All calculations were conducted with the VASP program [4], integrated within the MedeA software [5].

Band structures for heterostructures including CuO/Cu, Cu3N/Cu, Bi/$BaTiO_3$, Bi/$PbTiO_3$, Bi/HfO_2, La/$BaTiO_3$, and La/$PbTiO_3$ were computed considering spin-orbit interactions, and the Rashba parameter α_R, which measures the magnitude of spin-orbit splitting, was determined [6]. The study also examined how factors such as interfacial contact layers, drainage parameters, thickness, interface polarity, and ferroelectric polarization affect the Rashba parameter values.

The findings from this research can contribute to the development of functional materials for spintronics based on the properties of these compounds.

The calculations were supported by Kazan Federal University through the Laboratory of Computer Design of New Materials and Machine Learning.

[1] J. Zhou et al., Natl. Sci. Rev. **8,** nwaa176 (2021).
[2] E.I. Rashba, V.I. Sheka, Fiz. Tverd. Tela – Collected Papers (Leningrad) **II**, 162 (1959) [in Russian].
[3] A.D. Caviglia et al., Phys. Rev. Lett. **104**, 126803 (2010).
[4] G. Kresse and J. Furthmüller, Phys. Rev. B **54**, 11169 (1996).
[5] MedeA version 3.; MedeA is a registered trademark of Materials Design, Inc., San Diego, USA.
[6] Yu.A. Bychkov, E.I. Rashba, Sov. Phys. - JETP Lett. **39**, 78 (1984) [in Russian].

Spin-Hall effects in heteroepitaxial structure $Pd_{0.88}Fe_{0.12}$/Pt

Z.K. Pulotov[1], A.K. Kadikova[1], B.F. Gabbasov[1], I.V. Yanilkin[1], A.I. Gumarov[1], A.G. Kiiamov[1], L.R. Tagirov[1,2], R.V. Yusupov[1]

[1]Institute of Physics, Kazan Federal University, Kazan, Russian Federation
[2]Zavoisky Physical-Technical Institute, Kazan, Russian Federation

E-mail: pulotov.ru@gmail.com

Spin-Hall effects (SHE) are phenomena that arise from the coupling of charge and spin currents in media with strong spin-orbit interaction. SHE consists in the occurrence of a spin current during the flow of a charge current, which leads to a spatial redistribution of current carriers with oppositely directed spins. In elements of superconducting spintronics it is possible to redistribute the magnetization of the ferromagnetic layer without the involvement of a magnetic field. But the functioning of superconducting elements is possible only at cryogenic temperatures, thus one of the most promising materials for ferromagnetic layers is a solid solution of palladium and iron. Magnetic ordering in these materials occurs at temperatures much lower than the room temperature. We did not find any studies of spin-Hall effects in structures with magnetic layers based on Pd-Fe alloys, so the subject of the studies presented in the report was the SHE and inverse spin-Hall effects (ISHE) in the heteroepitaxial thin film structure $Pd_{0.88}Fe_{0.12}$/Pt.

Experiments have been carried out to observe direct and inverse spin-Hall effects in the heteroepitaxial structure $Pd_{0.88}Fe_{0.12}$/Pt. SHE is manifested in the observation of ferromagnetic resonance (FMR) spectra when, instead of modulating the magnetic field, an alternating electric current is passed through the sample. SHE leads in these conditions to the modulation of the magnetization value of the ferromagnetic layer and, accordingly, to the shift of the resonance line. In experiments with a $Pd_{0.88}Fe_{0.12}$/Pt bilayer heteroepitaxial structure, an estimate of an efficient magnetic field modulation of 50 mG was obtained when a current with an amplitude of 5 mA was passed through the heterostructure. However, the passage of a lateral current through the heterostructure, in addition to the occurrence of the desired spin-Hall effect, also leads to the generation of an alternating magnetic field due to electromagnetic induction. To establish the fact of SHE manifestation, the spatial distribution of the magnetic field generated by the electric current in the ferromagnetic layer $Pd_{0.88}Fe_{0.12}$ of the $Pd_{0.88}Fe_{0.12}$/Pt bilayer heteroepitaxial structure was calculated. Comparison of the magnetic field value obtained from the calculation with the effective modulation field showed that at least 70% of the effective modulation field is due to the SHE.

The inverse spin-Hall effect (ISHE) manifests itself in the voltage generation in the course of a spin-dependent scattering of electrons under spin pumping conditions. A voltage signal of the order of 1 μV was detected from the ISHE at temperatures from 20 to 150 K. A weak dependence of the signal amplitude on the sample temperature was observed. This, in our opinion, is due, on the one hand, to a decrease in magnetization with increasing temperature, thus reducing the spin current under conditions of spin pumping, and on the other hand, the sample is a metal, whose resistance increases with increasing temperature. Thus, the two effects cancel each other out in a given temperature range. The Hall angle for platinum was calculated, which at a temperature of 20 K was: $\alpha_{SHE} = (0.35 \pm 0.02)$ %. The Hall angle is the conversion coefficient between the charge and spin currents.

Magnetic inhomogeneities in Fe_3Al epitaxial thin films probed by FMR and time-resolved magnetooptics

A.Kh. Kadikova[1], A.V. Petrov[1], Kh.Sh.A. Taki [1], B.F. Gabbasov[1], A.I. Gumarov[1], I.V. Yanilkin[1], L.R. Tagirov[1,2], R.V. Yusupov[1]

[1]Institute of Physics, Kazan Federal University, Kazan, Russian Federation
[2]Zavoisky Physical-Technical Institute, Kazan, Russian Federation

e-mail: anelyakadikova11@gmail.com

Nowadays, the field of microelectronics called spintronics is developing rapidly. All spintronics elements are based on magnetically ordered materials – ferro-, ferri- and antiferromagnets. In this regard, one of the most important requirements for the materials used is high degree of homogeneity and low damping of the magnetization precession. The latter is characterized by the Gilbert damping constant α. In our presentation, we will apply the complementary methods of ferromagnetic resonance (FMR) and time-resolved magnetooptic spectroscopy to studies of magnetic inhomogeneities in Fe_3Al thin epitaxial films and demonstrate the richness of information extracted from their combination.

It will be shown that the magnetic homogeneity of films strongly depends on their composition and synthesis conditions, which manifests itself in the frequency spectrum and the damping rate of the magnetization precession. Also, an estimate of the Gilbert damping constant $\alpha = (2.84 \pm 0.17) \times 10^{-2}$ for a thin film (20 nm) $Fe_{70}Al_{30}$ is obtained. Thin films of the $Fe_{75}Al_{25}$ and $Fe_{70}Al_{30}$ compositions deposited at room temperature of the substrate and annealed at 400°C are magnetically inhomogeneous, which is revealed in at least two frequency components in the precession of magnetization and its fast damping. Films of the $Fe_{75}Al_{25}$ composition deposited at a substrate temperature of 400°C exhibit low–frequency (4-6 GHz) and high-frequency precession components (18-19 GHz) in a field of 0.3 T; we associate the latter with precipitates of α-Fe.

Non-resonant microwave absorption in topological insulator $Bi_{1.1-x}Sn_xSb_{0.9}Te_2S$

T.N. Enderova, V.O. Sakhin, R.B. Zaripov, E.F. Kukovitsky, Yu.I. Talanov

Zavoisky Physical-Technical Institute, Kazan, Russian Federation

e-mail: tenderova101@mail.ru

It was shown in [1] that electron paramagnetic resonance (EPR) technique could be effectively used to measure and study magnetoresistance phenomena in conducting materials. We have used EPR spectrometer with magnetic field modulation (Ω = 100 kHz), so detect only magnetic field dependent component of non-resonant microwave absorption (MWA) amplitude – dP/dH. The sample's magnetoresistance is proportional to the magnetic field dependence of MWA: $dP/dH \sim dR/dH$; hence magnetic field dependence of MWA can be interpreted as a direct measurement of the AC magnetoresistance.

The DC transport measurement method and technique of EPR were used to study magnetoresistance phenomena in topological insulator $Bi_{1.1-x}Sn_xSb_{0.9}Te_2S$ (x = 0.02; 0.04) (BSSTS). BSSTS is high-quality topological insulator with bulk energy gap $\Delta E \approx 150$ meV. At low temperatures ($T < 100$ K) surface conducting states contribute predominantly to sample conductivity [2]. Therefore, we focused our study on low temperatures and obtained magnetic field dependences of resistance $R(H)$ and the absorption derivative dP/dH (H) for our samples in temperature range 1.5 K ÷ 70 K. MWA data was obtained using EPR-spectrometer Elexsys E580 (Bruker) operating in the X frequency band. MWA data was integrated prior to comparison with results of DC resistance measurements. There is no disagreements in the observed magnetoresistance phenomena in DC transport properties and non-resonant MWA study.

In a low magnetic field (H < 600 Oe) in temperatures from 1.5 K to 20 K the impact of quantum interference on conductivity was detected in AC and DC transport measurements. This quantum effect corresponds to the case of weak antilocalization, which originates from destructive quantum interference of closed scattering paths of current carriers with strong spin-orbit coupling. Analysis of the magnetoresistance data obtained by both methods allows us to estimate the phase coherence lengths l_ϕ for both methods of transport properties measurements. For crystal with Sn x = 0.04 the temperature dependence of l_ϕ value was obtained in wide temperature range (1.5 ÷ 70 K). By analyzing $l_\varphi(T)$, it was established that electron-electron interaction is the main dephasing mechanism in a two-dimensional system of topological insulator BSSTS.

It should be expected that in large fields, where cyclotron frequency ω_c exceeds measurements frequency (spectrometer frequency) ω_0 $P(H)$ curve must follow $R(H)$ curve. For this reason, the magnetoresistance and magnetic field dependence of MWA were aligned at high field region. At some point with lowering magnetic field corresponding cyclotron frequency value becomes comparable to spectrometer frequency: $\omega_c \approx \omega_0 \approx 2\pi \cdot 9.6$ GHz. At this magnetic field $P(H)$ and $R(H)$ curves diverge. Using this fact, we were able to estimate cyclotron frequency and obtain effective mass of current carriers m^* from it. In our case for sample with Sn x = 0.04: $m^* = 0.02m_0$.

The research was supported by RSF grant No 21-72-20153.

[1] M. Golosovsky, Phys. Rev. B, **76**, 184414 (2007).
[2] S. Kushwaha, Nature Comm., **7**, 11456 (2016).

Combined equation of semiclassical spin dynamics and electron paramagnetic resonance

S.V. Demishev[1,2], A.V. Popov[1,2]

[1] Vereshchagin Institute for High Pressure Physics of the Russian Academy of Sciences, Troitsk, Moscow, Russia
[2] National Research University Higher School of Economics, Moscow, Russia

e-mail: arvipopov@edu.hse.ru

In a recent paper [1] it is shown that the equations of semiclassical spin dynamics with Landau-Lifshitz (LL) and Hilbert (G) relaxation terms are not equivalent in general case. When calculating the EPR spectrum, both variants of accounting for spin relaxation give a close line shape only in the limit of weak relaxation. In the case of significant dumping, the effect of the relaxation parameter on the maximum position of the absorption line turns out to be different, which may reflect different possible physical situations in systems with strong electron correlations [1].

In this work, we consider for the first time an equation for semiclassical magnetization **M** dynamics in a magnetic field **H** with a combined term representing a weighted sum of LL and G relaxation terms, $\mathbf{R}_{LL}=\lambda[\mathbf{M},[\mathbf{M},\mathbf{H}]]$ and $\mathbf{R}_G=\gamma\eta[\mathbf{M},d\mathbf{M}/dt]$:

$$\frac{d\mathbf{M}}{d\mathbf{H}}=\gamma[\mathbf{M},\mathbf{H}]-(\delta\cdot\mathbf{R}_{LL}+(1-\delta)\cdot\mathbf{R}_G), \qquad (1)$$

where $0\le\delta\le1$ sets relative contribution R_{LL}, и γ is gyromagnetic ratio. Following [1], it is possible to introduce relaxation parameters $\alpha_{LL}=\eta\chi_0\omega$ and $\alpha_G=\lambda\chi_0\omega/\gamma^2$ and, for simplicity, we will put $\alpha_{LL}=\alpha_G=\alpha$. In linear approximation $\mathbf{M}=\chi_0\mathbf{H}$, the calculation of absorbed power P for EPR in Faraday's geometry gives:

$$P=\chi_0 h_0^2\frac{\alpha\left(x^6+\left(1+(1-\delta)^2\alpha^2\right)x^4+(\delta\alpha x)^2\right)}{\left(x^4-\left(1-(1-\delta)^2\alpha^2\right)x^2-(\delta\alpha)^2\right)^2+(2\alpha x)^2}, \qquad (2)$$

where $x=\omega/(\gamma H_0)=\omega/\omega_H$ is the reduced frequency of microwave radiation and h_0 stands for the amplitude of variable magnetic field. The shape of the EPR line in coordinates $P/\chi_0h_0^2=f(x,\alpha)$ is shown in Fig.1 for case $\delta=0{,}5$ by three-dimensional graph and contour graph. It is visible that at $\alpha\sim2$ there is a sharp change in the position of the EPR line maximum x_{max}, at which the value of x_{max} changes 1.8 times. This effect is accompanied by an increase in EPR line width W and resulting $W(\alpha)$ turns out to be non-monotonous: there is a maximum on curve $W(\alpha)$in the range $2<\alpha<3$ (Fig. 1).

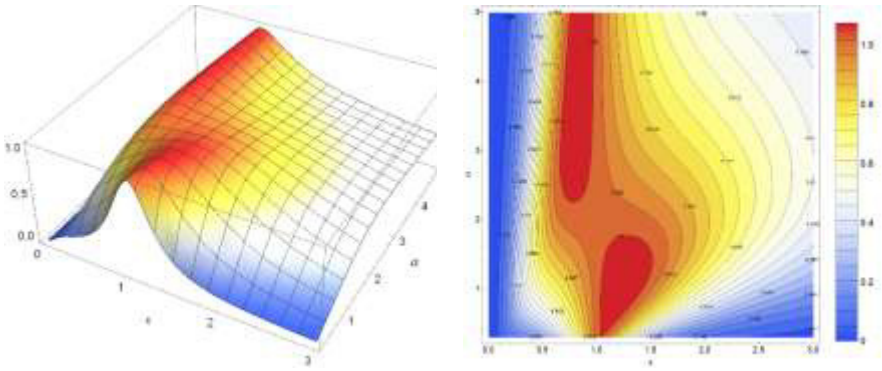

Fig. 1. The shape of the EPR line in coordinates $P/\chi_0 h_0^2 = f(x,\alpha)$ for case δ=0,5 by three-dimensional graph and contour graph.

The obtained result is of interest from the point of view of a new group of magnetic phenomena – spin-fluctuation transitions (SFT) [2], which are characterized by a sharp change in amplitude of magnetic fluctuations ΔM under variation of a control parameter. According to [1], a change in the relaxation parameter may be due to change in the amplitude of magnetic fluctuations. Then, in the model under consideration, a monotonous change in ΔM will lead to a maximum in EPR line width. Interestingly, this type of SFT was recently discovered in the spiral magnet MnSi [3].

1. S.V. Demishev, Appl. Magn. Reson. **55**, 1091 (2024).
2. S.V. Demishev, Physics – Uspekhi, **67**, 22 (2024).
3. S.V. Demishev et al., Sol. State Commun. **385**, 115501 (2024).

Description of unconventional superconductivity in the regime of strong fluctuations

F.M. Siraev, M.V. Avdeev, Yu.N. Proshin

Institute of Physics, Kazan Federal University, Kazan, Russian Federation

e-mail: siraevfail@mail.ru

Fluctuations are essential for understanding the transport and critical properties of low-dimensional materials with unconventional superconductivity, significantly influencing the material's behavior, especially near the critical temperature where superconductivity occurs [1]. Notable examples include the unusual temperature dependence of the superfluid density in ultrathin copper oxide films [2], hysteretic switching between superconducting and normal states with well-defined critical and retrapping currents in two-dimensional superconductors [3], and many other remarkable phenomena (see review [1]).

We propose and discuss an approach to describing the 2D d-wave superconducting state that accounts for fluctuations in the superconducting order parameter, where the pair interaction is governed by a superexchange potential.

Using variational perturbation theory, we derive an effective action for a mixed s- and d-wave two-component superconducting order parameter, analogous to the Coleman-Weinberg action [4]. The corresponding components are determined by minimizing the effective action.

Numerical calculations were performed using band parameters obtained from experimental photoemission data on YBCO compounds [5]. Within this framework, the temperature dependence of the order parameter amplitude and the critical temperature of the superconducting transition were calculated. It is shown that the critical temperature, renormalized due to fluctuations, is much lower than the value obtained in the mean-field approximation. The features of the temperature dependence of the order parameter near the superconducting transition are also discussed.

[1] T. Uchihashi, Superconductor Science and Technology **30**, 013002 (2016).
[2] I. Hetel, T.R. Lemberger, M. Randeria, Nature Physics **3**, 700 (2007).
[3] T. Uchihashi, P. Mishra P., Aono, T. Nakayama, Phys. Rev. Lett. **107**, 207001 (2011).
[4] S. Coleman, E. Weinberg, Phys. Rev. D **7**, 1888 (1973).
[5] M.R. Norman, Phys. Rev. B **63**, 092509 (2001).

Dipolar EPR Spectroscopy of Fullerene and Porphyrin Symmetric Pairs

R.A. Podarov[1,2], M.I. Kolokolov[1,2], E.V. Tretyakov[3], M.V. Fedin[1], O.A. Krumkacheva[1]

[1]International Tomography Center, SB RAS, Novosibirsk, Russia
[2]Novosibirsk State University, Russia
[3]N.D. Zelinsky Institute of Organic Chemistry, RAS, Russia

e-mail: podarov.r@tomo.nsc.ru

In this work, we introduce for the first time a dipole electron paramagnetic resonance (EPR) approach for measuring distances in symmetric non-orthogonal photoexcited spin pairs. Previous research has effectively explored spin pairs consisting either of a photoexcited triplet state of a molecule paired with a stable radical [1,2], or two photoexcited triplet states of different natures [3]. The subsequent phase involves examining a coupled system containing two photoexcited triplet states to potentially enhance the sensitivity of pulsed EPR techniques through the intensified hyperpolarized signal emanating from two identical components of the pair. Furthermore, such symmetrical systems are increasingly utilized in the efficient conversion of solar energy into electrical energy. Despite the theoretical efficiency limit of contemporary solar cells being only 34%, utilizing the singlet fission process in such symmetric spin pairs could elevate this efficiency to 44%. This increase is facilitated by the generation of two charge carriers rather than one, a process hindered by intersystem crossing (ISC) in spin pairs, which does not contribute to an efficiency gain in solar cells [4].

The aim of this work is to develop an approach for measuring nanometer-scale distances using electron paramagnetic resonance (EPR) in symmetric photoexcited spin pairs based on fullerene and porphyrin. The investigations were conducted using molecules of bisfullerene connected by a fluorinated linker, and pairs of chlorin e6 molecules in complex with human serum albumin.

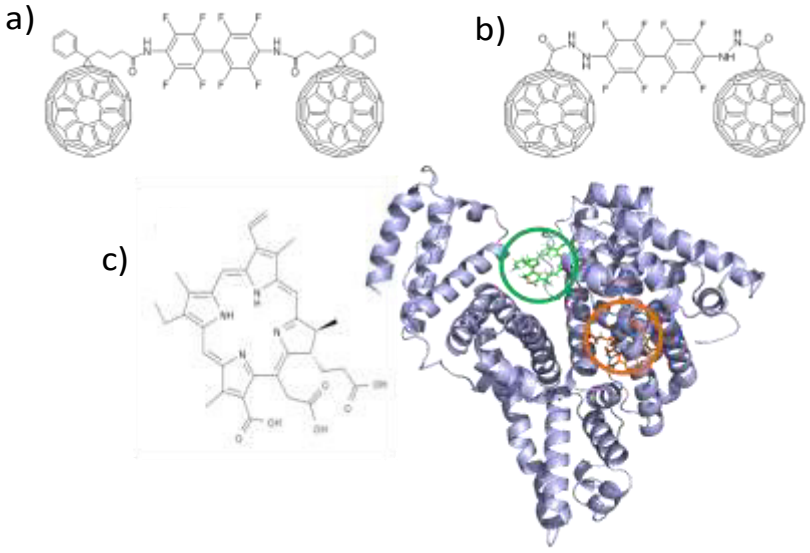

Fig. 1. Structures of the studied spin pairs: a) bisfullerene with a long linker, b) bisfullerene with a short linker, c) chlorine molecule e6 and its complex with human serum albumin.

The echo-detected spectra of the bisfullerene molecules revealed several noteworthy effects and distinctions compared to the monomeric form of PCBM. The spectrum of the bisfullerene was notably broader and featured a distinct set of spectral lines. Utilizing a theoretical framework that involves strongly interacting spins within fullerene pairs, coupled with considerably weaker dipolar interactions between the fullerenes, enabled the simulation of the echo-detected spectrum and the estimation of inter-fullerene distances using the point dipole approximation. Data derived from nutation experiments and subsequent modeling suggest that the formation of the two triplet states in the system under investigation occurs not via inter-combination conversion, but through the mechanism of singlet fission.

However, not all transitions within the triplet state spectra were accurately described by the existing model. During experiments with a delayed interval post-laser pulse, a spectral line emerged, associated with the coherence transfer of transitions having closely matched frequencies. Throughout the course of the experiments, a general decline in the intensity of the echo-detected spectrum was observed, alongside a notable peak at the center. Additionally, a resolution of the two extreme lines of the original triplet spectrum and a reversal in the sign of one of the spectrum lines were detected. These observed effects could be further modeled by considering an exchange interaction between the paired fullerenes.

We proposed a methodology for measuring distances in symmetric photoexcited spin pairs using the relaxation-induced dipole modulation enhancement (RIDME) pulsed EPR technique. The experimental label spacing determined in bisfullerene aligns with estimates derived from ED spectrum modeling. Additionally, this approach enabled the first-time measurement of the distance between two binding sites of chlorin e6 with albumin. The RIDME technique has thus proven effective for probing nanometer-scale distances in symmetric photoexcited spin pairs, including applications in biological systems. This method utilizes the high quantum yield of photoexcited triplet states and overcomes a significant limitation of dipolar methods—the presence of a broad echo-detected spectrum.

[1] O.A. Krumkacheva et al., Angewandte Chemie International Edition **58**, 13271 (2019).
[2] Di M. Valentin et al., Journal of the American Chemical Society **136**, 6582 (2014).
[3] A. Bertran et al., The journal of physical chemistry letters **12**, 80 (2020).
[4] M.B. Smith, J. Michl, Annu. Rev. Phys. Chem. **64**, 361 (2013).

EPR investigations of composite materials based on biocompatible polymers with calcium phosphates

A.A. Petrova[1], G.V. Mamin[1], F.F. Murzakhanov[1], I.V. Fadeeva [2], A.A. Forysenkova[2], M.R. Gafurov [1]

[1] Institute of Physics, Kazan Federal University, Kazan, 420029, Russian Federation, e-mail Petrovaalinakfu@gmail.com
[2] A.A. Baikov Institute of Metallurgy and Material Science, Russian Academy of Sciences, Leninsky Avenue 49, 119334 Moscow, Russia; fadeeva_inna@mail.ru

Since calcium phosphates (CP) constitute the primary mineral component of bone, composite materials containing CP are taken into consideration when treating bone tissue [1]. Materials with the required mechanical and biological qualities can be produced by combining the features of CP (hemostatic and antibacterial) with those of polymers (hydrophilicity, solubility, swelling). It's critical to comprehend the mechanism underlying the interaction between the polymer and calcium phosphates while developing composite materials.

To make composites, a variety of polymers, both synthetic and natural, can be used, including synthetic polyvinylpyrrolidone (PVP) and natural polysaccharide alginate (ALG) [2-4]. In this work we investigate composites containing synthetic CP hydroxyapatite (HA, $Ca_{10}(PO_4)_6(OH)_2$) and mentioned polymers prepared by freeze-drying of the gel by using photoinduced pulsed X- and W-band EPR spectroscopy.

In the temperature range of 100–300 K, no EPR signals were detected since the materials do not contain paramagnetic impurities at least within the sensitivity of the spectrometer. Under laser radiation, stable paramagnetic centers can be created (Figure 1) which disappear after several hours after switching off the laser.

Signal from PVP is mainly due to the isotropic hyperfine interaction of carbon-centered defects ($g_{PVP} = 2.0040$) with the polymer ^{14}N nuclei (Table 1). The EPR spectra of the irradiated HA and of the PVP-HA composite are mainly defined by the presence of the impurity of nitrates. The extracted EPR parameters correspond to NO_3^{2-} in B position (i.e., phosphate site) in the HA structure (Table 1).

Mixing HA with PVP-Alg somewhat changed the hyperfine interaction constants $A_\perp$ and $A_\parallel$ upwards, and also increased the distribution of the constants $\Delta A_\perp$ and $\Delta A_\parallel$ (Table 1). Analysis of changes in $A_\perp$ and $A_\parallel$ showed that the isotropic part of the hyperfine interaction increased by 3.7 MHz, which corresponds to an increase in the electron density at the nitrogen nucleus in the HA NO_3^{2-} complex by 2%. It can be assumed that, when HA is added ex situ, PVP-Alg molecules form a positively charged layer around the HA particles with the formation of a chemical bond, which increases the electron density in its near-surface layer. Due to electrical neutrality, the charge on the outer surface of the PVP-Alg shell will be negative.

Table 1. EPR parameters (axial components of *g*-factors, hyperfine values *A* and their distribution ΔA).

Sample	$g_\perp$	$g_\parallel$	$A_\perp$ MHz	$A_\parallel$ MHz	$\Delta A_\perp$ MHz	$\Delta A_\parallel$ MHz
PVP	2.0040	2.0040	2.75	2.75		
PVP-Alg	2.0022 (2)	2.0026(2)	38 ± 8	106 ± 10	-	-
HA	2.0011(1)	2.0052(1)	92.4 ± 0.5	186 ± 1	7 ± 1	12 ± 1
PVP-Alg-HA	2.0011(1)	2.0052(1)	93.6 ± 0.5	191 ± 1	13 ± 1	18 ± 1

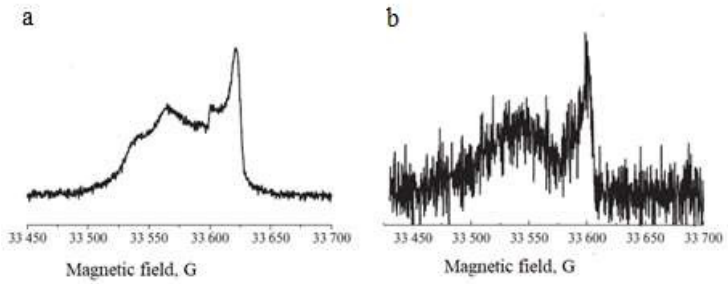

Fig. 1. W-band EPR spectra at T = 200 K under irradiation with light of 355 nm: a - PVP; b — HA–PVP composite.

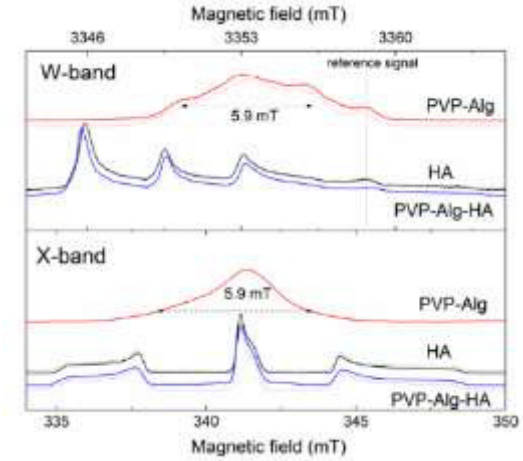

Fig. 2. Pulse EPR spectra for PVP-ALG (red lines), HA (black lines), and PVP-ALG-HA (blue lines) after X-ray irradiation (W-band at the top; X-band below). Dashed lines are the fits with the parameters given in Table 1.

The work is supported financially by Russian Science Foundation Grant No. 23-23-00640

[1] S.M. Barinov, Advances in chemistry **79**, 15 (2010).
[2] M. Furko et al., Coatings **13**, 360 (2023).
[3] I.V. Fadeeva, et al., Polymers **13**, 3989 (2021).
[4] A.A. Forysenkova et al., Materials **16**, 4478 (2023).

List of authors

Table of contents

T A B L E O F C O N T E N T S